

## One-Step Thermo-Chemical Synthetic Method for Nanoscale One-Dimensional Heterostructures

Guozhen Shen,<sup>\*,†</sup> Di Chen,<sup>‡</sup> and Chongwu Zhou<sup>†</sup>

Department of Electrical Engineering, University of Southern California, Los Angeles, California 90089, and Photocatalytic Materials Center, National Institute for Materials Science, Sengen 1-2-1, Tsukuba, Ibaraki 305-0047, Japan

Received March 25, 2008

Revised Manuscript Received May 3, 2008

Inspired by the discovery of carbon nanotubes in 1991,<sup>1</sup> enormous research efforts have been made on one-dimensional (1-D) nanostructures, such as nanowires, nanotubes, and nanobelts.<sup>2–5</sup> Among them, 1-D nanoscale heterostructures (HS) with modulated structure, compositions, and interfaces have become of particular interest,<sup>6–10</sup> which represent an important class of nanoscale building blocks with substantial potential for exploring and realizing novel device applications at the nanometer scale.<sup>6–10</sup>

Many methodologies have been developed for the synthesis of 1-D HS. For example, two-step or multistep catalytic-assisted metal–organic chemical vapor deposition methods and metal–organic vapor phase epitaxy methods have been extensively used to synthesize diverse 1-D HS, including core/shell, segmented, and hierarchical HS.<sup>6–8</sup> Using mixed source material, several 1-D HS were fabricated based on different mechanisms.<sup>9</sup> Other methods based on the solution chemical process, electrospinning, lithography, and so forth were also developed to get 1-D HS.<sup>10–13</sup> Every

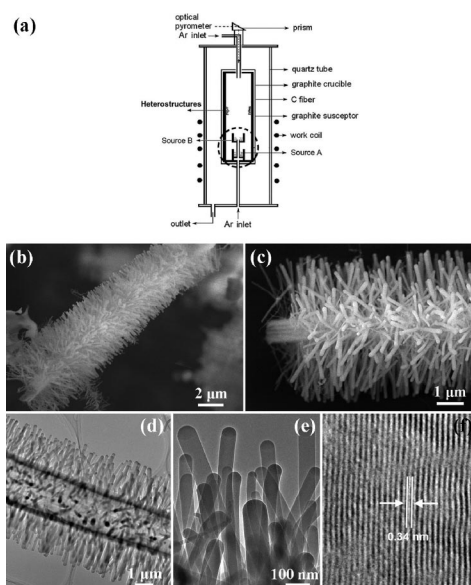


**Figure 1.** (a) Schematic illustration of the furnace used in the experiments. (b, c) SEM images of as-synthesized hierarchical C/SiO<sub>2</sub> microtube/nanowire HS. (d) TEM image of a hierarchical HS. (e) TEM image of the branched SiO<sub>2</sub> nanowires. (f) TEM image taken from the core C microtubes, showing clear lattice fringes.

methodology has its advantages and disadvantages from different view points. It is still challenging to develop a simple and generic method to rationally synthesize 1-D nanoscale HS.

Herein, we present a simple one-step thermo-chemical synthetic method for the synthesis of a variety of 1-D HS, including hierarchical C/SiO<sub>2</sub> microtube/nanowire, GaP/ZnS nanowire/nanowire, GaP/CdS nanowire/nanowire HS, and core/shell Zn/ZnS, Ge/ZnS nanowires. Our synthetic method is a very simple one with many benefits. It is a general method to produce a large quantity of 1-D HS. With a judicious choice of source materials and careful control of experimental parameters, this simple method can even be extended to synthesize other complex HS, such as self-assembled raspberry-like GaS spheres decorated with Bi nanoparticles.

The one-step thermo-chemical synthetic method for 1-D HS involves a vertical induction furnace<sup>14</sup> as shown in Figure 1a. The key feature of the experimental setup is the usage of a specially designed crucible system as marked with a dashed circle in Figure 1a. The crucible system is composed of two graphite or boron nitride crucibles connected with a graphite pipe. The bottom crucible for source A, used to

\* Corresponding author. E-mail: guozhens@usc.edu.

<sup>†</sup> University of Southern California.

<sup>‡</sup> National Institute for Materials Science.

- (1) Iijima, S. *Nature* **1991**, *354*, 56.
- (2) (a) Pan, Z. W.; Dai, Z. R.; Wang, Z. L. *Science* **2001**, *291*, 5510. (b) Kong, X. Y.; Ding, Y.; Yang, R.; Wang, Z. L. *Science* **2004**, *303*, 1348.
- (3) (a) Hu, J. T.; Odom, T. W.; Lieber, C. M. *Acc. Chem. Res.* **1999**, *32*, 435. (b) Cui, Y.; Wei, Q. Q.; Park, H. K.; Lieber, C. M. *Science* **2001**, *293*, 1289.
- (4) Goldberger, J.; He, R. R.; Zhang, Y.; Lee, S. W.; Yan, H.; Choi, H. J.; Yang, P. D. *Nature* **2003**, *422*, 599.
- (5) (a) Shen, G. Z.; Chen, D. *J. Am. Chem. Soc.* **2006**, *128*, 11762. (b) Liu, B.; Zeng, H. C. *J. Am. Chem. Soc.* **2004**, *126*, 16744.
- (6) (a) Wu, Y.; Fan, R.; Yang, P. D. *Nano Lett.* **2002**, *2*, 83. (b) Dick, K.; Deppert, K.; Larsson, M. W.; Martensson, T.; Seifert, W.; Wallenberg, L. R.; Samuelson, L. *Nat. Mater.* **2004**, *3*, 380.
- (7) (a) Park, W. I.; Yi, G. C.; Kim, M.; Pennycook, S. J. *Adv. Mater.* **2003**, *15*, 526. (b) Hsu, Y. J.; Lu, S. Y. *Chem. Commun.* **2004**, 2102.
- (8) (a) Lathon, L. J.; Gudiksen, M. S.; Wang, C. L.; Lieber, C. M. *Nature* **2002**, *420*, 6911. (b) Qian, F.; Li, Y.; Gratecak, S.; Wang, D. L.; Barrelet, C. J.; Lieber, C. M. *Nano Lett.* **2004**, *4*, 1975. (c) Xiang, J.; Vidan, A.; Tinkham, M.; Westervelt, R. M.; Lieber, C. M. *Nat. Nanotechnol.* **2006**, *1*, 208.
- (9) (a) Shen, G. Z.; Bando, Y.; Gao, Y. H.; Golberg, D. *J. Phys. Chem. B* **2006**, *110*, 14123. (b) Shen, G. Z.; Ye, C.; Golberg, D.; Hu, J.; Bando, Y. *Appl. Phys. Lett.* **2007**, *90*, 073115. (c) Hu, J.; Bando, Y.; Liu, Z.; Golberg, D.; Zhan, J. *J. Am. Chem. Soc.* **2003**, *125*, 11307.
- (10) Ostermann, R.; Li, D.; Yin, Y. D.; McCann, J. T.; Xia, Y. N. *Nano Lett.* **2006**, *6*, 1297.
- (11) (a) Milliron, D. J.; Hughes, S. M.; Cui, Y.; Manna, L.; Li, J.; Wang, L.; Alivisatos, A. P. *Nature* **2004**, *340*, 190. (b) Yang, H. G.; Zeng, H. C. *J. Am. Chem. Soc.* **2005**, *127*, 270. (c) Mokari, T.; Banin, U. *Chem. Mater.* **2003**, *15*, 3955.
- (12) (a) Lao, J. Y.; Wen, J. G.; Ren, Z. F. *Nano Lett.* **2002**, *2*, 1287. (b) Sun, S.; Yang, D.; Zhang, G.; Sacher, E.; Dodelet, J. P. *Chem. Mater.* **2007**, *19*, 6376. (c) Maynor, B. W.; Li, J.; Lu, C.; Liu, J. *J. Am. Chem. Soc.* **2004**, *126*, 6904.
- (13) (a) Stoermer, R. L.; Keating, C. D. *J. Am. Chem. Soc.* **2006**, *128*, 13243. (b) Love, J. C.; Urbach, A. R.; Prentiss, M. G.; Whitesides, J. *J. Am. Chem. Soc.* **2003**, *125*, 12696. (c) Martin, B. R.; Dermody, D. J.; Reiss, B. D.; Fang, M.; Lyon, L. A.; Natan, M. J.; Mallouk, T. E. *Adv. Mater.* **1999**, *11*, 1021.
- (14) (a) Shen, G. Z.; Bando, Y.; Ye, C.; Yuan, X.; Sekiguchi, T.; Golberg, D. *Angew. Chem., Int. Ed.* **2006**, *45*, 7568. (b) Ma, R.; Bando, Y.; Sato, T.; Kurashima, K. *Chem. Mater.* **2001**, *13*, 2965.

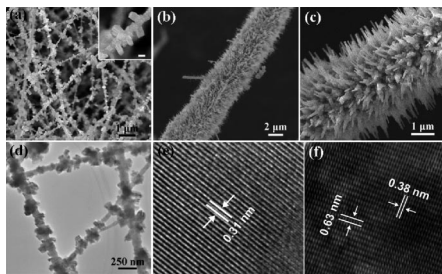


**Figure 2.** SEM images of the hierarchical GaP/ZnS nanowire/nanowire HS after reaction for (a) 30 min and (b, c) 2 h. (d) TEM image of a hierarchical nanowire. HRTEM images of (e) the core GaP nanowire and (f) branched ZnS nanowire.

produce stem nanowires of desired HS, was set in the center of the heating zone of the furnace, while the position of the upper crucible for source B, used to produce secondary/branched nanowires of HS, is adjustable according to different source materials. To get the desired HS, several factors should be considered when setting the position of upper crucible, such as the melting point of source B and the gas flow rate. In most cases, the graphite crucible was used to promote the evaporation of the source materials, while in some cases, the BN crucible was used to avoid the chemical reaction between graphite and the source materials. The detailed experiments and crucible system setup can be found in the Experiment Section in Supporting Information. Furthermore, a high-frequency vertical induction furnace instead of the conventional tube furnace favors the formation of diverse HS. A main factor is that temperature increases very fast for the induction furnace. For example, the temperature can increase from room temperature to 1400 °C within 10 min. Faster temperature increase is believed to be favorable for rapid evaporation of sources, which is very important for the vapor growth of nanostructures.<sup>9,14</sup> Besides, the vertical induction furnace has two gas inlets from both the bottom and the top, which is also important for HS synthesis. Our experimental setup fully utilizes the temperature degradation of the furnace and makes the synthetic process finishing within one step.

The first kind of 1-D HS synthesized here is the hierarchical HS. Figure 1b,c demonstrates the hierarchical C/SiO<sub>2</sub> microtube/nanowire HS, which consisted of numerous branched nanowires wrapped around a microtube. The TEM image shown in Figure 1d also shows the hierarchical structure, consistent with the SEM results. The clear brightness contrast indicates the inner part is of tubular structure. Figure 1e is a TEM image of the branched nanowires, which have uniform lengths of 2–3 μm and diameters of 50–100 nm. The clear contrast variations between the tips and the nanowires suggest that the body and the tip of the nanowire may consist of different materials. Energy-dispersive electron spectrometry (EDS) was used to check the compositions of the hierarchical HS, and the data suggest the core microtubes are C microtubes and the branched nanowires are SiO<sub>2</sub> nanowires with Sn tips. Figure 1f shows an HRTEM image taken from the core C microtubes. The clearly resolved lattice fringe is about 0.34 nm, corresponding to the (002) lattice parameter of graphitic carbon.

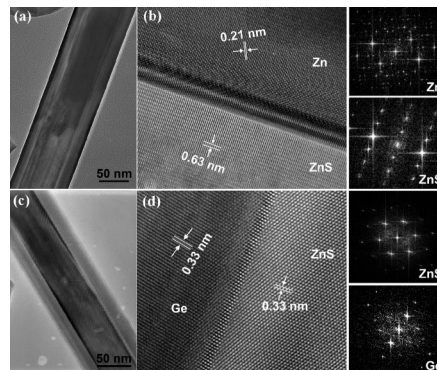


**Figure 3.** (a, b) TEM and HRTEM images and FFT patterns of core/shell Zn/ZnS nanowires. (c, d) TEM and HRTEM images and FFT patterns of core/shell Ge/ZnS nanowires.

Figure 2a–c shows the SEM images of another kind of hierarchical heterostructure, GaP/ZnS nanowire/nanowire heterostructure, synthesized at different times, and indicates the formation process of the HS. At the initial stage of growth (30 min, Figure 2a), long nanowires decorated with low density short nanowires are produced. After reaction for 1 h, the branched nanowires grew longer and the density is higher (Supporting Information, Figure S3). At 2 h, the density of the branched nanowires becomes much higher and trepan-like hierarchical HS are formed (Figure 2b,c). Figure 2d is a TEM image of the HS formed after 30 min. Long nanowires decorated with small nanowires can be clearly seen from the image, consistent with the SEM results in Figure 2a. EDS spectra taken from the core nanowire and the branched nanowire show that they are GaP nanowire and ZnS nanowire, respectively. An HRTEM image taken on the core GaP nanowire (Figure 2e) shows that it is single-crystalline and the spacing of the lattice planes perpendicular to the nanowire long axis is 0.31 nm, consistent with the (111) planes of cubic GaP. The HRTEM image at the branched small ZnS nanowire gives lattice fringes of 0.63 nm perpendicular to the long axis and 0.38 nm along the long axis, corresponding to the [0001] and [01 $\bar{1}$ 0] lattice fringes of wurtzite ZnS. These data indicate that the core GaP nanowires are single crystals with preferred growth direction along the (111) orientations and the branched ZnS nanowires are single crystals grown along the [0001] direction. Using a similar process, we can also synthesize hierarchical GaP/CdS HS.

The present method is also useful for 1-D core/shell HS. Figure 3a depicts a TEM image of the core/shell Zn/ZnS nanowires. A core/shell structure was easily seen from the contrast variations between the core and the inner part. EDS analysis indicates that it was core/shell Zn/ZnS nanowires. An HRTEM image shown in Figure 3b was used to investigate the microstructures of the Zn core and the ZnS shell, as well as the interface between them. For the upper part, the lattice fringe is about 0.21 nm, corresponding to the (101) plane of hexagonal Zn phase. The measured lattice fringe for the bottom part is 0.63 nm, consistent with the [0001] plane of the wurtzite ZnS phase. The corresponding fast Fourier transform (FFT) patterns of both parts are shown in the Figure 3b inset, revealing the single crystal natures of both the Zn core and the ZnS shells. Due to the large lattice

mismatch between hexagonal Zn and wurtzite ZnS, high density defects, like stacking faults, exist within the interface of the core and the shells (Figure 3b). Core/shell Ge/ZnS nanowires were also synthesized and Figure 3c is a TEM image of a typical core/shell Ge/ZnS nanowire. Its HRTEM image is depicted in Figure 3d. The marked lattice fringes are 0.33 nm for the Ge core and 0.33 nm for the ZnS shell, respectively. They are obviously consistent with the (111) plane of the cubic Ge phase and the (100) plane of the hexagonal ZnS phase. The interface between the core and the shell is a perfect one and appears to be very homogeneous and atomically sharp. It is easy to explain because of the perfect lattice match between Ge and ZnS. Corresponding FFT patterns of both core and shell were also shown in the Figure 3d inset, which also reveal their single crystal nature.

On the basis of the above results, a general vapor–solid (VS) mechanism was proposed to explain the formation of diverse HS since no catalyst was used in most cases. At high reaction temperature, *source A* is evaporated directly or reacts with graphite to general vapors for the growth of main nanowires. At the same time, *source B* is also evaporated (due to the precise control of position of crucible) to generate vapors, which is transferred to low temperature region and deposit on the main nanowires to form secondary/branched nanowires. After reaction finished, 1-D HS are produced. Using GaP/ZnS HS as an example, GaP in crucible A was evaporated at high temperature and the generated GaP gases were transferred to low temperature region and deposit on the inner wall to form GaP nanowires. At the same time, ZnS in crucible B was also evaporated to generate ZnS vapors, which was also transferred to low temperature region and directly deposited on GaP nanowires to form GaP/ZnS HS. Although the formation of C/SiO<sub>2</sub> HS is also mainly governed by VS mechanisms for the growth of stem C tubes, catalyst Sn are necessary to promote the growth of secondary SiO<sub>2</sub> nanowires, which means a vapor–liquid–solid (VLS) mechanism.

The present one-step thermo-chemical method is also useful to be extended to synthesize other complexes with a judicious choice of source materials and careful control of experimental parameters. Here, self-assembled raspberry-like GaS spheres decorated with Bi nanoparticles were used as an example, and the corresponding discussions are as follows. Figure 4a shows a SEM image of the product synthesized from GaN (Source B) and Bi<sub>2</sub>S<sub>3</sub> (Source A). The product possesses an interesting hierarchical raspberry-like morphology. The morphology can be clearly seen from a high-

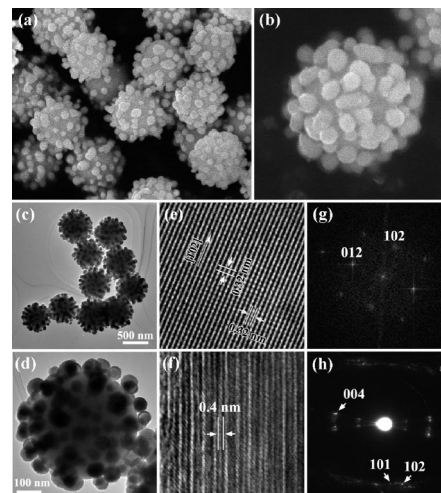


**Figure 4.** (a, b) SEM and (c, d) TEM images of the hierarchical GaS spheres decorated with numerous Bi nanoparticles. (e) HRTEM image and (g) FFT pattern of the Bi nanoparticle. (f) HRTEM image and (h) SAED pattern of the GaS sphere.

magnification SEM image in Figure 4b. The raspberry-like sphere consists of a sphere core with many small nanoparticles decorated on it. TEM images of the raspberry-like products were demonstrated in Figure 4c,d, which is similar to the SEM results. EDS analysis reveals that the core is GaS and the decorated small nanoparticles are Bi (Supporting Information, Figure S7). The measured lattice is 0.32 nm for Bi and 0.4 nm for GaS, corresponding to the (012) plane of hexagonal Bi phase and the (004) plane of a hexagonal GaS crystal. The inset FFT (Figure 4g) and SAED patterns (Figure 4h) are consistent with the HRTEM results.

In conclusion, a simple one-step thermo-chemical synthetic method was developed to synthesize a variety 1-D HS. The synthetic 1-D HS include hierarchical HS and core/shell HS. The successful synthesis of 1-D HS makes it possible to investigate their corresponding properties, such as electronic and optoelectronic properties. Devices like field-effect transistors are expected to be fabricated based on single 1-D heterostructures. With a judicious choice of source materials and careful control of experimental parameters, this method was extended to synthesize other complex HS.

**Supporting Information Available:** Experimental procedures, more SEM, TEM, HRTEM images, and EDS spectra of the produced 1-D HS (Figure S1–S7) (PDF). This material is available free of charge via the Internet at <http://pubs.acs.org>.

CM8008557